Modeling a fluid / solid transition in snow weak layers
Application to snow avalanche release

François Louchet[1,3,*], Alain Duclos[2], and Stephane Caffo[2]
[1]Data-avalanche.org, 284 chemin du Pré Roudon, 38410 St Martin d'Uriage, France
[2]Data-avalanche.org, 15 rue de la Buidonnière, 73500 Aussois, France
[3]Laboratoire de Glaciologie et de Géophysique de l'Environnement, UJF-Grenoble 1/CNRS, BP 96, 38402 St Martin d'Hères Cedex, France

Abstract: A transition between solid and a fluid-like phases was evidenced and studied in the material made of loose ice crystals involved in snow avalanche release. A kinetic model is proposed, showing the existence of a transition between a fluid phase and a solid structure, for a given stress level. The model accounts for the observed characteristics of the transition, and may be applied to a number of other granular materials. It is applied here to slab avalanche release, and predicts avalanching for slopes steeper than a critical value, estimated around 30^o in typical snowcover conditions.

KEYWORDS: slab, triggering, weak layer, collapse, shear, whumpf.

1 INTRODUCTION

Some amazing properties of weak layers were evidenced and reported in the Davos ISSW conference [Duclos 2009]. After summarizing these field observations that evidenced a transition between a solid and a granular fluid phase in the weak layer material, the present paper aims at modeling this transition in terms of kinetics of bond failure and reconstruction, and at discussing the possible consequences on snow avalanche release.

2 FIELD OBSERVATIONS AND EXPERIMENTS

Experiments were conducted at the Orelle ski resort, on april 26th, 2008, at an elevation of 3230m, with an air temperature of -1^{o}C. Shortly after being carefully collected from the weak layer and deposited on a steeply inclined board, the material (depth hoar, or faceted snow) behaves as a granular fluid (F) made of grains that flow in a way similar to dry rice. However, when left undisturbed for a few seconds, it clots into a granular solid (S). When mechanically disturbed again (e.g. mechanical shock), the same aggregates may turn back to the F phase if the disturbance is large enough. [1]

Corresponding author address: Francois Louchet, Data-avalanche.org, 284 chemin du Pré Roudon, 38410 St Martin d'Uriage, France;
Tel: +33 (0)649555475;
email: f.louchet@gmail.com

This transition is studied using a pendulum made of a steel sphere (A) with a mass m = 0.68kg, hung to a fixed point. Another pendulum (B) of similar length is made of a bottle of about 0.954 dm^3, whose bottom has been removed, positioned upside down, and hung close to A. After closing the lid, the bottle is filled with the granular material. After 15 to 30 s, the lid is carefully removed. Since the material had enough time to clot, it does not flow out of the bottle. Pendulum A is then drawn some distance aside, and released in order to knock the bottle. The test is repeated from increasing distances between A and B, i.e. increasing heights H, until the shock energy is large enough to trigger the S to F transition, and to allow the material to flow out of the bottle, which occurs for H values roughly between 3 and 4.5 cm. Measuring the kinetic energy of A at triggering (equal to mgH) allows an estimate of the energy necessary to bring the clotted system to fluid state, found around 200 to 300 J/m^3.

3 MODELING

We describe the fluid medium as a composite made of solid clusters (clotted "rice grains" aggregates) embedded in a granular "liquid" (free dry "rice grains"), and we compute the rate at which solid clusters form, grow or disaggregate during shear displacements that control contact times for both grain-cluster and grain-grain interactions. We label the proportion of grains in the fluid by N. The proportion of grains resp. in solid clusters and at solid/liquid interfaces are N_s and N_i, such

that $N+N_s+N_i=1$. We assume $Ni << (N, N_S)$, which gives:

$$N_S \approx 1-N \tag{1}$$

The interface particle proportion scales as $N_s^{2/3}$, giving:

$$N_i \propto {N_S}^{2/3} \approx (1-N)^{2/3} \tag{2}$$

Let us first consider that the system is in a fluid state, loaded at imposed strain rate. The liquid phase is fed by particles taken from cluster interfaces; this process is driven by fluid shear, and its kinetics therefore assumed to be proportional to the strain rate $\dot{\gamma}$ and to interface grain proportion N_i.

On the other hand, grains are taken out from the liquid phase as they form bonds with either other "liquid" grains (cluster nucleation) or interface grains (cluster growth).

The reaction kinetics of such a bond formation is taken proportional to the contact time between "liquid" and "interface" grains, that obviously scales as $(1/\dot{\gamma})$. Using eq. (2), the global reaction kinetics is therefore given by:

$$\begin{aligned} dN/dt &= AN_i\,\dot{\gamma} - \frac{B}{\dot{\gamma}}\left(\frac{N}{2}+N_i\right) \\ &= A(1-N)^{2/3}\,\dot{\gamma} - \frac{B}{\dot{\gamma}}\left[\frac{N}{2}+(1-N)^{2/3}\right] \end{aligned} \tag{3}$$

where A and B are constants.

Actually, it may be easier to argue in terms of imposed stress (i.e. slope and slab weight) than of imposed strain rate. In order to transform eq (3) into an imposed stress equation, we need to define a viscosity η characteristic of the fluid phase only, that relates the stress τ and the strain rate by $\dot{\gamma} = \tau/\eta$.

For this purpose we use here Einstein's expression [Einstein 1905], writen in our notations as:

$$\eta = \eta_0 \frac{1+N_S/2}{1-2N_S} = \eta_0 \frac{3-N}{2(2N-1)} \tag{4}$$

where η_0 is the residual viscosity of the pure liquid i.e. without any solid cluster.
From eqs.(3) and (4), we have:

$$\begin{aligned} dN/dt &= A\frac{2\tau}{\eta_0}\frac{(1-N)^{2/3}(2N-1)}{(3-N)} \\ &- B\frac{\eta_0}{2\tau}\frac{3-N}{2N-1}\left[\frac{N}{2}+(1-N)^{2/3}\right] \end{aligned} \tag{5}$$

In the following, we will be only interested in the time evolution of N, i.e. the sign of dN/dt, which is the same as that of:

$$\xi(N) \equiv \frac{dN}{dt}\frac{1}{B}\frac{2\tau}{\eta_0} \tag{6}$$

$$= \frac{A}{B}\left(\frac{2\tau}{\eta_0}\right)^2\frac{(1-N)^{2/3}(2N-1)}{(3-N)} - \frac{3-N}{2N-1}\left[\frac{N}{2}+(1-N)^{2/3}\right]$$

$$= \Sigma\,\frac{(1-N)^{2/3}(2N-1)}{3-N} - \frac{(3-N)\left(\frac{N}{2}+(1-N)^{2/3}\right)}{2N-1}$$

with:

$$\Sigma = \frac{A}{B}\left(\frac{2\tau}{\eta_0}\right)^2 = C\left(\frac{2\tau}{\eta_0}\right)^2 \tag{7}$$

where C is a constant.

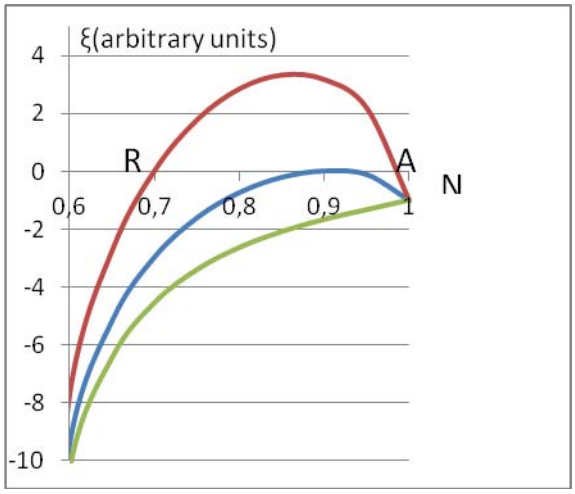

Figure 1. $\xi(N)$ curves (arbitrary units) for different Σ values: Σ =60 (red), Σ = Σ_c = 21.5 (blue), Σ =1 (green).

Fig. 1 shows typical $\xi(N)$ curves parametrized by Σ. The system behaviour drastically changes for a critical Σ value $\Sigma_c \approx 21.5$. For $\Sigma < \Sigma_c$ indeed, (i.e. low stresses and (or) large viscosities), $\xi(N)$ is always negative. Starting from any initial N value, N continously decreases and the fluid clots into the solid phase at $N=0$. By

contrast, for $\Sigma > \Sigma_c$ (i.e. large stresses and (or) small viscosities), the curve exhibits a maximum and intersects the N axis for two N values, N_R and N_A ($N_R < N_A$), that are the fixed points of the system.

N_A is an attractor, since an upwards fluctuation of N results in a negative dN/dt value, that brings the N value back to N_A, and conversely for a downwards fluctuation. A similar argument shows that N_R is a repulsor. Both fixed points merge for $\Sigma = \Sigma_c$ (blue curve), corresponding to a N value $N_c \approx 0.9$. As a consequence, starting from any N value smaller than N_R drives the system to the solid phase $N=0$, whereas starting from $N > N_R$ brings the system to the attractor N_A. Since $N_c \approx 0.9$, the stable fluid contains no more than 10% of particles belonging to solid clusters. This proportion decreases even further as Σ increases.

4 COMPARISON WITH FIELD OBSERVATIONS:

Such results can now be compared to the board and bottle experiments. Let us start from a fluid already flowing on an inclined board. If the slope of the board is steep enough, the driving force (gravitational shear stress) is large, and Σ may exceed the threshold value Σ_c. In this case, the system is trapped around the attractor N_A, and the fluid goes on flowing. As the slope is gradually reduced, so is the shear stress, Σ decreases, the attractor shifts towards slightly lower N values, but the fluid keeps flowing until Σ reaches the Σ_c value for which the two fixed points merge. Beyond this point, $\xi(N)$ becomes negative everywhere, and the fluid suddenly clots into the solid phase.

Let us now start from an unloaded clotted solid ($N = 0$). We first load the system up to a given stress corresponding to a given Σ value. Since $\xi(N=0)<0$, the system remains solid. We can change the initial conditions giving a mechanical shock in order to break bonds and temporarily increase the N value. If Σ is smaller than Σ_c (moderately slanted slope), $\xi(N)$ being always negative, the system clots back again. On the opposite, for Σ values larger than Σ_c (steeply inclined board), two situations may be contemplated. A weak shock may bring N to a value smaller than N_R. In this case, despite the large Σ value, $\xi(N)$ remains negative, and the system clots back again. By contrast, a stronger shock may bring N to a value larger than N_R, i.e. to the attraction basin of N_A. In this case, $\xi(N)$ is positive and the system readily becomes fluid at $N=N_A$, and starts flowing down. For very large Σ values, N_R being very small, a tiny shock may destabilize the system. The bottle experiment can be explained in quite a similar way.

5 APPLICATION TO SNOW SLAB AVALANCHE RELEASE:

5.1. Assumptions and definitions

The above observations and model may have an obvious application to snow avalanche release, regarding basal crack nucleation and propagation in interfaces between slabs and substrates. Local loadings on slabs, due to skiing or snowboarding or to explosive devices, may be responsible for the initiation of a so-called basal crack that may further expand due to the weight of the slab itself.

Previous simplified models considered the stability of such basal cracks under shear loading, essentially based on Griffith's concepts [Louchet 2000, 2001, 2002] or on more complicated but equivalent ones [McClung 1979, 1981, Bazant 2003]**.** However, the weak layer is a non-compact medium that may easily collapse under compressive loads, as already suggested by Jamieson and Schweizer [Jamieson 2000] and clearly shown recently using Propagation Saw Tests (PST) [Gauthier 2006, 2008, Heierli 2008a]. Basal cracks are therefore initiated by a local combination of collapse and shear failure modes of the weak layer, that can vary between the two limiting cases of pure shear and pure collapse [Heierli 2008b]. In the general case, collapse of the WL results in a fluid F phase layer prone to downslope glide. The question is whether the F phase will remain fluid and allow avalanching, or clot into a solid S phase, that would stop the triggering process. This question is now discussed in terms of the above model.

In the present analysis of triggering mechanisms, we shall use the following definitions:

h: "real" slab thickness, i.e. measured perpendicular to the slab

$h_{//}$: slab thickness measured vertically

w: thickness of the collapsible part of the WL measured perpendicular to the slab

$w_{//}$: thickness of the collapsible part of the WL measured vertically
δ: residual weak layer thickness after collapse, measured perpendicular to the slab
w+δ: weak layer thickness before collapse, measured perpendicular to the slab

We first consider an infinite slope, and we label α the local slope angle with respect to horizontal. Assuming no wind conditions, we consider that snow falls vertically. As a consequence, the resulting slab has a constant vertical thickness $h_{//}$, corresponding to a "real" thickness $h=h_{//} \cos \alpha$ measured perpendicular to the slope, that decreases for increasing slope angles. We also consider that during snow metamorphism, the WL grows along the maximum temperature gradient direction, resulting in a WL thickness (w+δ) (measured perpendicular to the slab/substrate interface), independent of slope angle.

Avalanche release results from two successive stages, that will be examined hereafter.

5.2. Weak layer collapse

This first stage takes place under a combination of compressive and shear load components. A local WL collapse results in a reduction of slab thickness from *w+δ* to *δ*. Once initiated, the collapsed zone may extend under a "driving force" equal to the work of the slab weight per square meter *ρgh* along the vertical collapse distance $w_{//}$. From above definitions, this "driving force" can be written:

$$\rho g h w_{//} = \rho g (h_{//} \cos\alpha)(w/\cos\alpha) = \rho g h_{//} w \quad (8)$$

Since $h_{//}$ is determined by the snow fall, and *w* by weather and snow metamorphism, both are independent of slope angle, and so is the driving force for collapse.

The critical radius of the collapsed zone (in Griffith's sense), above which it may extend spontaneously, can be easily computed as a balance between the driving force on the one hand, and the resistant force opposing crack extension, determined by the energy required to collapse the WL, on the other hand.
Such a driving force for collapse was calculated [Heierli 2008] under the assumption of a constant *h* (and not $h_{//}$), which would lead to fairly different conclusions than ours. However, both their driving force and ours coïncide on flat terrain, where $h = h_{//}$. Our remark above (eq. (8)) that the collapse "driving force" in the case of vertical snowfall is independent of slope angle allows us to generalize to all kinds of slopes their results on flat terrain.
One of their results was that the critical size is fairly low, with a typical value on flat terrain of a few decimeters. This result is valid in our case for all slope angles. This means that a small local collapse initiated by a skier for instance is likely to rapidly propagate along the whole WL, whatever the slope.

5.3. Weak layer shearing and downslope slide of the slab

The question is now whether this collapsed zone will result in avalanche release or not. Since the WL is in the collapsed state, this second stage is driven by the shear component of the load only. Two different situations may be contemplated, depending on whether the strain rate $\dot{\gamma}$ (resp. the shear stress *τ*) in the WL is smaller or larger than the critical strain rate value $\dot{\gamma}_c$ (resp. the critical shear stress value $\tau_c = \eta \dot{\gamma}_c$) as defined in section 3.

i) for sufficiently large slope angles and slab weights, the resulting shear strain rate $\dot{\gamma}$ (resp. shear stress *τ*) in the WL is larger than the critical shear strain rate $\dot{\gamma}_c$ (resp. critical shear stress τ_c). In this case, the strain rate is sufficiently large to maintain the WL in the F state, and the slab can slide down.

ii) for small slope angles and slab weights, the conditions are such that the strain rate is lower than $\dot{\gamma}_c$, the WL readily clots into the S phase, and the triggering process is stopped.

We shall illustrate now these two cases on a numerical example close to typical field conditions, comparing applied and critical stresses for different slope angles. We found in section 3 that the F/S transition takes place for a critical *Σ* value $\Sigma_c \approx 21.5$. However, as we do not have numerical figures for C and η_0 involved in eq. (7), nor any values from specifically dedicated experiments, we shall make here very crude estimates from literature,

in order to obtain nothing but an order of magnitude for the critical stress τ_c.

The critical shear stress can be indirectly estimated from crack face friction experiments (Rutsch Block or PST) [Van Herwijnen 2009]. In some of their experiments, the slab comes quickly to a rest (e.g. in their fig. 4) instead of accelerating downslope (in their fig. 2), which is a clear illustration of a very sharp F/S transition. Their experiments C5 and C1 for instance exhibit resp. an accelerating and a clotting behaviour, both for a slope angle of 33°. Taking α≈33° and a slab depth around h≈30 cm (see their fig. 1), and assuming a typical slab density of 300 kg/m^3, the transition should occur for a critical shear stress: $\tau_c \approx 480$ Pa. Such a critical stress has to be compared with the shear stress experienced by the WL:

$$\tau = \rho g h \sin\alpha = \rho g h_{//} \cos\alpha \sin\alpha = \frac{\rho g h_{//}}{2} \sin 2\alpha \qquad (9)$$

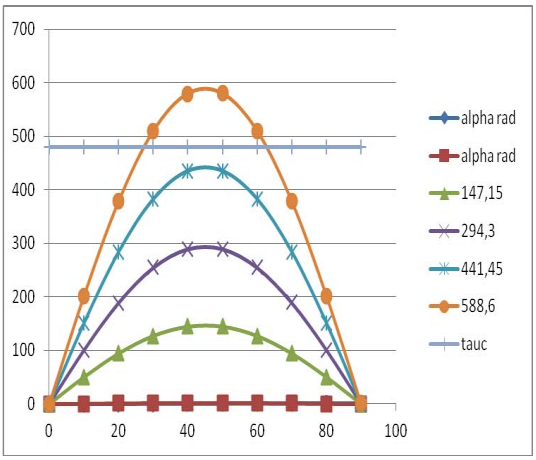

Figure 2. Comparison of the critical shear stress τ_c with the shear stress τ experienced by the weak layer for a slab density of 300kg/m3, and for slab depths (measured vertically) of 10cm (triangles), 20cm (crosses), 30cm (stars) and 40cm (disks). In this case, avalanche release cannot occur for slab depths less than 30cm. For a depth of 40 cm, avalanching becomes possible above a slope angle of 28°, and up to a slope angle of 62° (see text).

This is illustrated in fig. 2, for different slab depths ranging from 10 to 40 cm. The *sin2α* function responsible for the inverted U-shaped shear stress curves results from our assumption that snow falls vertically in average, giving a constant vertical $h_{//}$ depth. It goes to zero at both zero and 90°, since on moderate slopes the actual slab weight is large but its shear component tends to zero, whereas on steepest slopes the shear component is large, but the amount of snow tends to zero. The horizontal line shows the critical stress value τ_c = 480 Pa in this particular example. It intersects the shear stress experienced by the WL for slab depths larger than about 33cm. For a slab depth of 40 cm, avalanches can be triggered for slope angles larger than 28°, and up to 62°.

Within the limits of our assumptions, consequences are as follows:

i) moderate slopes: large normal-slope stresses result in WL collapse and associated whumpfs; slope-parallel motion quickly comes to a rest due to clotting of the F phase, and avalanches are not released.

ii) intermediate slopes: The shear stress and the associated shear strain rate are large enough to keep the WL in the F state, and the avalanche is likely to be released.

iii) steep slopes: same conclusions as in i). Such a prediction may seem to be surprising, but crown cracks are often observed to open at the junction between intermediate and very steep slopes.

5.4. Stability of the collapsed weak layer after clotting:

Another question is whether the WL may stay at rest for ever after collapse and subsequent clotting (as described above), or destabilize again upon further mechanical loading due for instance to another skier.

For this purpose, we compare typical values of the skier's kinetic energy with the estimate given in section 2 of the energy necessary to bring the clotted system back to the fluid state.

A skier of 80 kg, with a velocity of 30 km/h = 8 m/s, has a kinetic energy of about 2.5 kJ. We assume that such an energy is entirely released in the WL during a sudden stop or a fall, which is clearly an overestimate.

In comparison, we take a 5mm thick WL (e.g. [Heirli 2008b]), on a surface of the order of the theoretical Griffith's size for nucleation of a shear crack, with a typical

value of 100m [Louchet 2000][2]. The corresponding WL surface is about $10^4 m^2$, and the involved WL volume about $50 m^3$. Taking a "fluidization" energy about 250 J/m^3 (see section 2), we find a required destabilization energy of 12.5 kJ, significantly larger than the estimate of the skier's kinetic energy.

As a consequence, further WL destabilization after clotting seems fairly unlikely (though not strictly impossible) under such conditions.

6 DISCUSSION

In agreement with [Van Herwijnen 2009], our model predicts a sharp transition between whumpfing and avalanching, but in contrast with [Van Herwijnen 2009], this sharp transition is not discussed here in terms of a continuous evolution of a Coulomb crack-face friction but in terms of a phase transition from a fluid to a solid phase in the collapsed WL. In other words, it is not expressed in terms of friction but in terms of viscosity. The huge viscosity discontinuity between these two phases (10 to about 10^5 Pa.s) evidenced in field experiments [Duclos 2009] confirms indeed that a friction analysis based on Coulomb friction is questionable. The transition is shown to depend on shear strain rate, i.e. on both shear load and WL thickness.

The above results stand for the ideal case of infinite, smooth and uniform slopes. In real slopes, the shear stress computed above may be reduced by boundary conditions (terrain roughness, stauchwalls, gully banks, …). Such a decrease (and distortion) of the applied shear stress curve of fig. 2 shows that the critical angle α_c for avalanche release is expected to increase, and the slope may become totally safe when the shear stress curve entirely lies below the critical shear stress τ_c (horizontal line).

In addition, snow transportation by wind, more particularly in the vicinity of ridges, may increase snow depth and result in a distortion of the inverted U-shaped curves, in particular for large slope angles, favouring avalanche triggering on such slopes.

[2] Owing to a smaller driving force, the critical Griffith's size in pure shear is significantly larger than in combined "collapse-shear" mode.

Finally, slab release not only requires downslope slab shift, but also slab rupture, i.e. crown crack opening [Louchet 2000, Faillettaz 2004]. This last point is scarcely mentioned in slab release models. Crown crack opening takes place when the increasing tensile load experienced by the slab during downslope slab glide exceeds slab strength. In this case the avalanche is actually released. But if for some reason (system geometry, variability of snow mechanical properties, …) the tensile load transferred to the slab top due to its downslope shift never reaches the slab tensile strength, slab release would not take place.

7 SUMMARY AND CONCLUDING REMARKS

The present model is based on our original observation that collapsed weak layers are made of a granular material that can experience sudden phase transitions from a granular fluid phase F to a granular solid one S, and conversely.

Evolution equations considering shear-rate dependent erosion and aggregation kinetics of ice grains reproduce such a behaviour, and give a physical basis to field experiments.

The model is then applied to the slab avalanche triggering problem. It predicts a sharp transition between whumpfing and avalanching, controlled by the strain rate of the collapsed weak layer. In standard conditions, avalanching becomes possible when the typical slope angle exceeds a value between 10^o and 40^o (fig. 2).

Such results, obtained for infinite, smooth and uniform slopes, are likely to be modified on real slopes, where terrain roughness, stauchwalls or other boundary conditions may shift the critical slope angle up to higher values. By contrast, snow transportation that may increase slab depth at places is likely to favour avalanche triggering.

Owing to its general character, our model may be used in other cases where granular slurries may undergo abrupt viscosity changes upon mechanical loading. In particular, the present approach may be relevant for investigating permafrost stability against building construction [Vakili 1991, Crory 1982], and, more hypothetically, to account for Mars "channel" formation [Cabrol 1992], ascribed to fluidization of frozen permafrost under meteoritic impacts.

8 REFERENCES

Bazant Z.P., Zi G. & McClung D., 2003. Size effect law and fracture mechanics of the triggering of dry snow slab avalanches, J. of Geophys. Research 108(B2) 2119: 13.1-13-11.

Cabrol N.A. and Grin E.A., 1992. Martian Channel Networks: a revised Strahler approach for quantitative morphometry. In Lunar and Planetary Inst., Workshop on the Martian Surface and Atmosphere Through Time, p. 28-29.

Crory F.E., 1982. Piling in frozen ground,J. of the Technical Councils of the American Society of Civil Engineers, 108 (1), pp. 112-124.

Duclos A., Caffo S., Bouissou M., Blackford J.R., Louchet F.and Heierli J., 2009. Granular Phase Transition in Depth Hoar and Facets: A New Approach to Snowpack Failure. Poster presentation, International Snow Science Workshop, Davos, Switzerland, 27 september-2 october 2009.

Einstein A., 1905. On the movement of small particles suspended in stationnary liquids required by the molecular-kinetic theory of heat. Ann. Phys. 17: 549-560.

Faillettaz J., Louchet F. and Grasso J-R., 2004. Two-threshold model for scaling laws of non-interacting snow avalanches, Physical Review Letters 93(20): 208001,1-4.

Gauthier D. and Jamieson B., 2006. Evaluation of a prototype field test for fracture and failure propagation propensity in weak snowpack layers, Cold Regions Science and Technology 51 (2-3): 87-97.

Gauthier D. and Jamieson B., 2008. Fracture propagation propensity in relation to snow slab avalanche release: Validating the Propagation Saw Test, Geophysical Research Letters 35: L13501-13504.

Heierli J., van Herwijnen A., Gumbsch P., Zaiser M., 2008a. Anticracks: a new theory of fracture initiation and fracture propagation in snow. In: C. Campbell, S. Conger and P. Haegeli (editors) Proceedings ISSW 2008. International Snow Science Workshop, Whistler BC, Canada, 21 September-27 September 2008, pp. 9-15.

Heierli, J., P. Gumbsch and M. Zaiser, 2008b. Anticrack Nucleation as Triggering Mechanism for Snow Slab Avalanches, Science 321 (5886): 240-243.

Jamieson J.B. and Schweizer J., 2000. Texture and strength changes of buriedsurface-hoar layers with implications for dry snow-slab avalanche release. J.Glaciol. 46 (152): 151-160.

Louchet F., 2000. A simple model for dry snow slab avalanche triggering, Comptes Rendus à l'Académie des Sciences, 330, 821-827.

Louchet F., 2001. Creep instability of the weak layer and natural slab avalanche triggerings.Cold Regions Science and Technology, 33: 141-146.

Louchet F., Faillettaz J., Daudon D., Bédouin N., Collet E., Lhuissier J. and Portal A-M., 2002. Possible deviations from Griffith's criterion in shallow slabs, and consequences on slab avalanche release, Nat. Hazards Earth Syst. Sci., 2: 157-161.

McClung D., 1979. Shear fracture precipitated by strain softening as a mechanism of dry slab avalanche release, J. of Geophys. Research 84(B7): 3519-3526.

McClung D., 1981. Fracture mechanical models of dry slab avalanche release, J. of Geophys. Research 86(B11): 10783-10790.

Vakili J., Leighton and Assocs. Inc.,1991 Slope stability problems in open pit coal mines in permafrost regions. International Arctic Technology

Conference, 29-31 may 1991, Anchorage, Alaska (USA), pp. 29-31

Van Herwijnen A. and Heierli J., 2009. Measurement of crack-face friction in collapsed weak snow layers, Geophys. Research Letters36,L23502: 1-5.

9 ACKNOWLEDGEMENTS

The authors gratefully acknowledge Dr. J. Heierli for assistance in designing and carrying out the field experiments, and Dr. J. Heierli and Dr. J. Blackford for helpful discussions.